

## Categorization of non-mass-like breast lesions detected by MRI

Naomi Sakamoto · Mitsuhiro Tozaki · Kuniki Higa · Yuko Tsunoda · Tomoko Ogawa ·  
Satoko Abe · Shinji Ozaki · Masaaki Sakamoto · Tomoko Tsuruhara · Naoko Kawano ·  
Takako Suzuki · Norie Yamashiro · Eisuke Fukuma

Received: 23 April 2007 / Accepted: 1 October 2007 / Published online: 22 January 2008  
© The Japanese Breast Cancer Society 2008

### Abstract

**Background** Breast MR imaging has emerged as a highly sensitive modality for the imaging of breast tumors. However, a standardized method of interpretation of lesions showing non-mass-like enhancement does not exist. The purpose of this study was to analyze the features of non-mass-like breast lesions detected by MRI, and to establish a standardized method of interpretation to allow categorization of these lesions.

**Methods** A retrospective review was performed for 102 consecutive nonpalpable mammographically occult, non-mass-like lesions detected by MRI that had undergone ultrasound-guided vacuum-assisted biopsy. MR imaging was performed on a 1.5-Tesla system. The distribution patterns were classified into three categories as follows: single quadrant/solitary lesion (linear), single quadrant/grouped lesion (focal, regional, segmental), and multiquadrant lesion (multiple regions, diffuse). The presence of a ductal pattern was assessed in the enhancing lesions after the tumor distribution had been decided. In addition to the BI-RADS-MRI descriptors, the presence of clustered ring enhancement was also assessed in heterogeneous enhancing lesions. We divided non-mass-like lesions into those with a small (category 3a), moderate (category 3b), or substantial (category 4) likelihood of malignancy.

**Results** The features with the highest positive predictive value (PPV) for cancer were clustered ring enhancement (67%) ( $P = 0.004$ ), a branching-ductal pattern (38%)

( $P = 0.003$ ), and clumped architecture (20%). The PPV for cancer of a linear-ductal pattern was 11% (1/9). All lesions showing multiquadrant distribution, linear-non-specific lesion, non-branching pattern with homogeneous and stippled internal architectures, and heterogeneous lesion without clustered ring enhancement were diagnosed as benign.

**Conclusion** Non-mass-like breast lesions detected on MRI showing a clustered ring enhancement, a branching-ductal pattern, and clumped architecture should be evaluated further by biopsy (category 4), while lesions not showing these characteristics may be observed without unnecessary intervention (category 3a). Lesions showing a linear-ductal pattern may be followed carefully or evaluated by biopsy as needed (category 3b).

**Keywords** Non-mass-like lesions · MRI · Categorization

### Introduction

Breast MR has emerged as a highly sensitive modality for the imaging of breast tumors [1–7]. Differences in MR enhancement characteristics between benign and malignant lesions are believed to reflect differences in vascularity, vessel permeability, and extracellular diffusion space.

The recently published BI-RADS (Breast Imaging Reporting and Data System) by the American College of Radiology included the first edition of MRI lexicons [8]. First, lesion configuration is determined as either a focal mass enhancement (space-occupying lesion) or non-mass-like enhancement. Among lesions showing non-mass-like enhancement, segmental or clumped linear and ductal enhancement were reported to be more frequent in ductal carcinoma in situ (DCIS) than in benign lesions [9–11].

N. Sakamoto (✉) · M. Tozaki · K. Higa · Y. Tsunoda ·  
T. Ogawa · S. Abe · S. Ozaki · M. Sakamoto · T. Tsuruhara ·  
N. Kawano · T. Suzuki · N. Yamashiro · E. Fukuma  
Breast Center, Kameda Medical Center, 929 Higashi-cho,  
Kamogawa, Chiba 296-8602, Japan  
e-mail: n.sakamoto@kameda.jp

However, a standardized method of interpretation of lesions showing non-mass-like enhancement does not exist.

The goal of the present study was to analyze the features of non-mass-like breast lesions detected by MRI, and to establish a standardized method of interpretation to allow categorization of these lesions.

## Materials and methods

### Patients

Retrospective review was performed for 102 consecutive nonpalpable mammographically occult, MRI-detected non-mass-like lesions that had undergone ultrasound-guided vacuum-assisted biopsy (US-VAB) from January 2003 to March 2005. The patients age ranged from 31 to 83 years, with a mean age of 49 years.

Indications for MR examination included need for further work-up in 59 cases (58%); screening in 23 cases (23%); follow-up for another lesion after biopsy in 11 cases (11%); preoperative assessment of extent of disease in 5 cases (5%); and 4 symptomatic lesions (nipple discharge) (4%).

### Breast US and US-VAB

Screening breast US and second-look US examinations were performed with the patient in the supine position with the arms raised, using an Aloka model SSD-5500 ultrasound system (Aloka Co., Japan) with a 10 MHz linear-array probe. US-VAB was performed using 11-gauge probes (Mammotome<sup>®</sup>, Johnson & Johnson, Japan). Successful VAB of the lesions was assessed by MRI after biopsy.

### MR imaging

MR imaging was performed using a 1.5-T system (Vision; Siemens Medical Solutions, Erlangen, Germany). All patients were examined in a prone position using a double breast coil. A sagittal fat-suppressed T2-weighted fast spin-echo sequence was performed with the following parameters: TR/TE, 4750/120; field of view, 16 cm; matrix size, 256 × 150; slice thickness, 6 mm without a gap.

Three-dimensional fat-suppressed fast low angle shot (FLASH) imaging was obtained before and four times after the bolus injection of 0.1 mmol Gd-DTPA/kg at a rate of 2 mL/s, followed by a 20-mL saline flush using an automatic injector. Both the breasts were examined in the coronal plane on the first-, second-, and fourth-phase

dynamic images, acquired at 30 s, 90 s, and 4.5 min, respectively. The MR imaging parameters were as follows: TR/TE, 29.1/4.0; flip angle, 30°; field of view, 25 cm; matrix, 256 × 128; receiver bandwidth, 244 Hz/pixel; and time of acquisition, 60 s. The section thickness varied, depending on the size of the breast, and ranged from 2.5 to 5 mm without a gap. The affected single breast was sagittally examined on images obtained in the third phase at 3 min (section thickness, 3.0 mm and time of acquisition, 120 s).

### Image interpretation

One experienced breast radiologist (MT) evaluated all the cases; the radiologist was unaware of any clinical information or the histopathological diagnosis.

First, the distribution patterns were classified into three categories as follows: single quadrant/solitary lesion (linear), single quadrant/grouped lesion (focal, regional, segmental), and multiquadrant lesion (multiple regions, diffuse). Secondly, the presence of a “ductal pattern” was assessed in the enhancing lesions (positive or negative). Thirdly, internal enhancement (homogeneous, heterogeneous, stippled, clumped, reticular) was evaluated. Fourthly, in addition to the BI-RADS-MRI descriptors, the presence of clustered ring enhancement [12] was assessed in heterogeneous enhancing lesions (positive or negative).

The distribution of the lesions was analyzed on coronal images. The presence of a ductal pattern was evaluated on sagittal images acquired at 3 min. The pattern of internal enhancement, including clustered ring enhancement, was evaluated on all images.

### Categorization of non-mass-like lesions

The fourth edition of BI-RADS included the subcategorization of category 4 lesions [8]. With the results of the previous study [13], positive predictive values (PPVs) of lesions categorized as BI-RADS 4 were as follows: category 4a, 6% (6/102); category 4b, 15% (17/110); and category 4c, 53% (48/91). In the present study, we divided category 3 and 4 lesions into those with a small (category 3a), moderate (category 3b), or substantial (category 4) likelihood of malignancy (Table 1). Category 3a is used for findings thought to have a less than a 2% chance of malignancy and for which a 6-month follow-up may be implemented. Category 3b suggests that the percentage of likelihood of malignancy in the evaluated lesion ranges from 2 to 15%. Category 4 is used for findings that require biopsy.

**Table 1** Categorization of MRI-detected non-mass-like lesions

Category [8]	PPV% [13]	Categorization in this study
3	<2	<2%: 3a (6-month follow-up suggested)
4a	6	2–15%: 3b (short interval follow-up suggested)
4b	15	
4c	53	≥16%: 4 (biopsy should be considered)

### Statistical analysis

For analysis of group differences from dichotomous variables, Fisher's exact test was employed. A *P*-value of less than 0.05 was considered to indicate a statistically significant difference.

## Results

### US-VAB and histology

Screening breast US showed no abnormal findings. On the second-look US, hypoechoic nodules or hypoechoic areas or ductlike structures were observed in the location of the lesions on the MRI in all cases. The US findings were suggestive of “probably benign” lesions, without any characteristics suspicious of malignancy. In a case that was evaluated as a multiquadrant lesion on the MRI, biopsy was performed of one site that represented these US findings. The average number of cores of US-VAB was 14. MRI conducted after the biopsy revealed a success rate of US-VAB of the lesions of 91% (93/102). There were nine residual lesions (unsuccessful biopsy) that were followed without additional biopsy. No additional biopsy was performed on these lesions, as they exhibited a constant appearance on the MRI over a 2-year follow-up period and were, therefore, considered to be benign.

Among 93 lesions, histologic analysis showed carcinoma in 10 (10%), of which 9 (90%) were DCIS and 1 (10%) was invasive ductal carcinoma. The remaining 83 lesions were benign, and included atypical ductal hyperplasia ( $n = 1$ ), intraductal papilloma ( $n = 1$ ), fibroadenoma ( $n = 2$ ), fibrocystic disease ( $n = 69$ ), fibrosis ( $n = 7$ ), mastitis ( $n = 2$ ), and granuloma ( $n = 1$ ).

### MR findings

Table 2 shows the frequencies of the morphological parameters, including clustered ring enhancement. The most frequent morphological finding among the benign

**Table 2** MR imaging parameters in non-mass-like enhancement cases

Descriptor	Benign ( $n = 92$ )	Malignant ( $n = 10$ )	<i>P</i> -value <sup>a</sup>
Distribution modifiers			
Single quadrant/solitary lesion			
Linear	10 (11)	1 (10)	NS
Single quadrant/grouped lesion			
Focal area	34 (37)	6 (60)	NS
Regional	19 (21)	0	NS
Segmental	16 (17)	3 (30)	NS
Multiquadrant lesion			
Multiple regions	1 (1)	0	NS
Diffuse	12 (13)	0	NS
Ductal pattern			
Linear-nonspecific	$n = 79$	$n = 10$	
Linear-ductal	2 (2.5)	0	NS
Non-branching	8 (10)	1 (10)	NS
Branching-ductal	61 (77)	4 (40)	NS
Branching-ductal	8 (10)	5 (50)	0.003
Internal enhancement (non-branching)			
Homogeneous	$n = 61$	$n = 4$	
Heterogeneous	2 (3)	0	NS
Heterogeneous	37 (61)	2 (50)	NS
Stippled, punctate	14 (23)	0	NS
Clumped	8 (13)	2 (50)	NS
Clustered ring enhancement (heterogeneous)			
Positive	$n = 37$	$n = 2$	
Negative	1 (3)	2 (100)	0.004
Negative	36 (97)	0	

Percentages are shown in parentheses

NS Not significant

<sup>a</sup> The Fisher's exact tests

lesions was a non-branching pattern (77%), followed by heterogeneous internal enhancement (61%); on the other hand, a focal distribution (60%), and a branching-ductal pattern (50%) were the most frequent findings in malignant lesions. None of the distribution patterns showed a statistically significant association with benign or malignant lesions. The features with the highest PPV for carcinoma were clustered ring enhancement (67%,  $P = 0.004$ ) (Fig. 1), a branching-ductal pattern (38%,  $P = 0.003$ ) (Fig. 2), and clumped architecture (20%). The PPV for cancer of a linear-ductal pattern was 11% (1/9).

Figure 3 illustrates the interpretation model proposed by Tozaki et al. [11]. All lesions showing multiquadrant distribution (multiple regions, diffuse), linear-nonspecific lesion, non-branching pattern with homogeneous and stippled internal architecture, and heterogeneous lesion without clustered ring enhancement were diagnosed as benign.

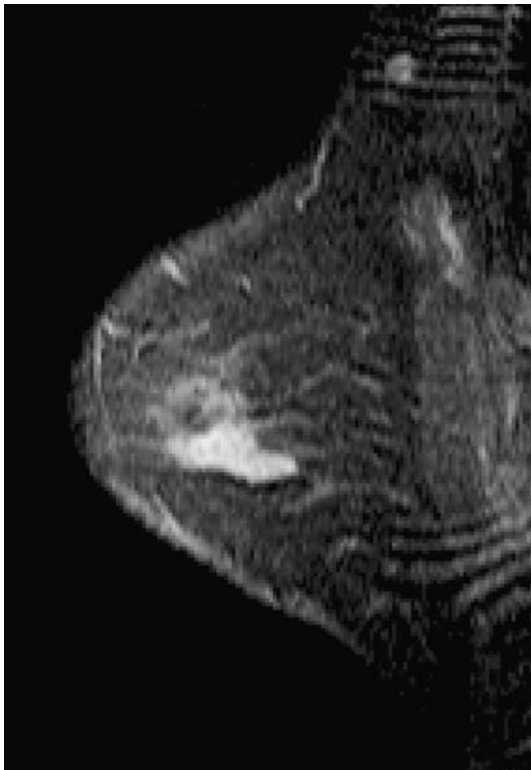


**Fig. 1** A 48-year-old woman with a history of breast biopsy in lower inner quadrant of right breast. MRI was performed for follow-up of the lesion. MRI shows focal enhancement in upper inner region of right breast. Lesion indicates heterogeneous enhancement inside of which minute ring enhancements are seen clustered (clustered ring enhancement). Histologic evaluation of the US-VAB specimen revealed ductal carcinoma in situ

## Discussion

Although breast MRI has emerged as a highly sensitive modality for the diagnosis of breast tumors, the reported specificity is lower [1–7]. Specificity can potentially be improved by careful analysis of lesion morphology and kinetics. An international group of breast MRI experts supported by the American College of Radiology and the Office of Women’s Health had been developing a lexicon for breast MRI [14, 15]. According to the BI-RADS-MRI lexicon [8], the lesion’s configuration, classified as mass enhancement (space-occupying lesion) or non-mass-like enhancement, should be determined first. Many cases of DCIS are detected as non-mass-like enhancements and exhibit a segmental or ductal distribution and a clumped internal architecture [9–11]. This standardized terminology facilitates interpretation and communication among breast radiologists. However, a standardized method of interpretation for the categorization of lesions showing non-mass-like enhancement does not exist. Categorization of non-mass-like breast lesions detected by MRI may reduce the frequency of unnecessary biopsy.

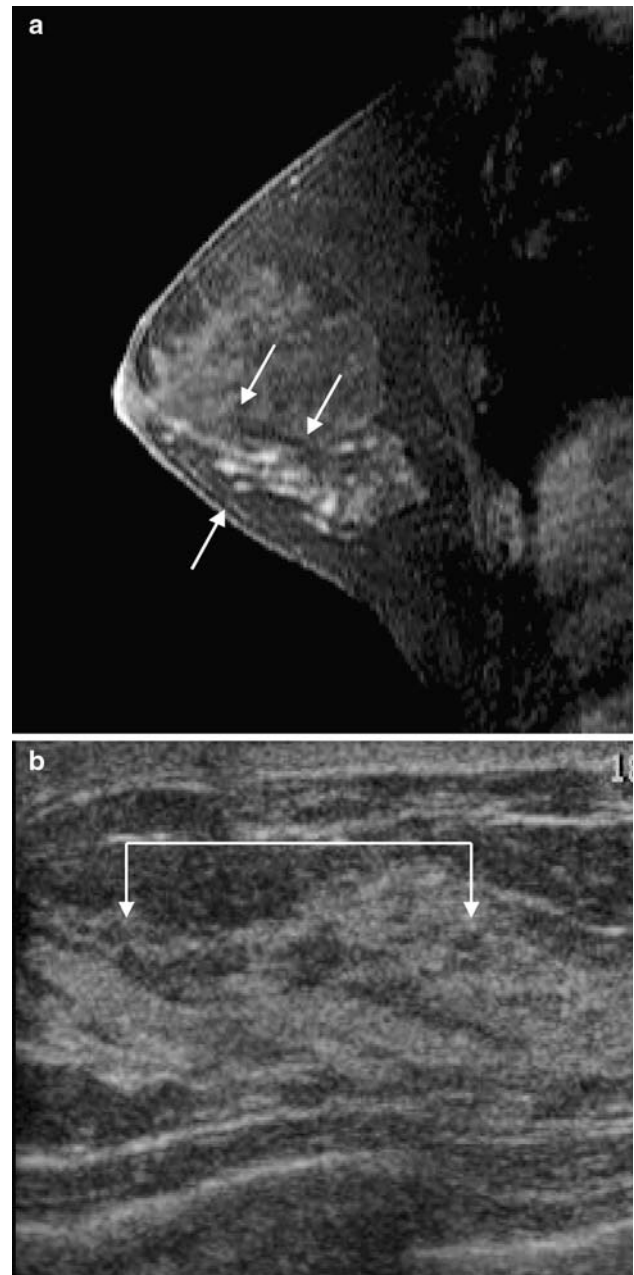


**Fig. 2** A 39-year-old woman with breast cancer in upper outer quadrant of left breast. MRI was performed for preoperative assessment of extent of disease. **a** MRI shows branching ductal enhancement in lower region of right breast (arrows). **b** Second-look US shows hypoechoic ductlike structures (arrows) in the location of the lesions on the MRI. Histologic evaluation of the US-VAB specimen revealed atypical ductal hyperplasia

With respect to the morphological parameters, the features with the highest PPV for carcinoma were clustered ring enhancement (67%) ( $P = 0.004$ ), a branching-ductal pattern (38%) ( $P = 0.003$ ), and clumped architectures (20%). Liberman et al. [9] reported that the feature with the highest PPV were segmental or clumped internal enhancement and ductal enhancement for non-mass-like

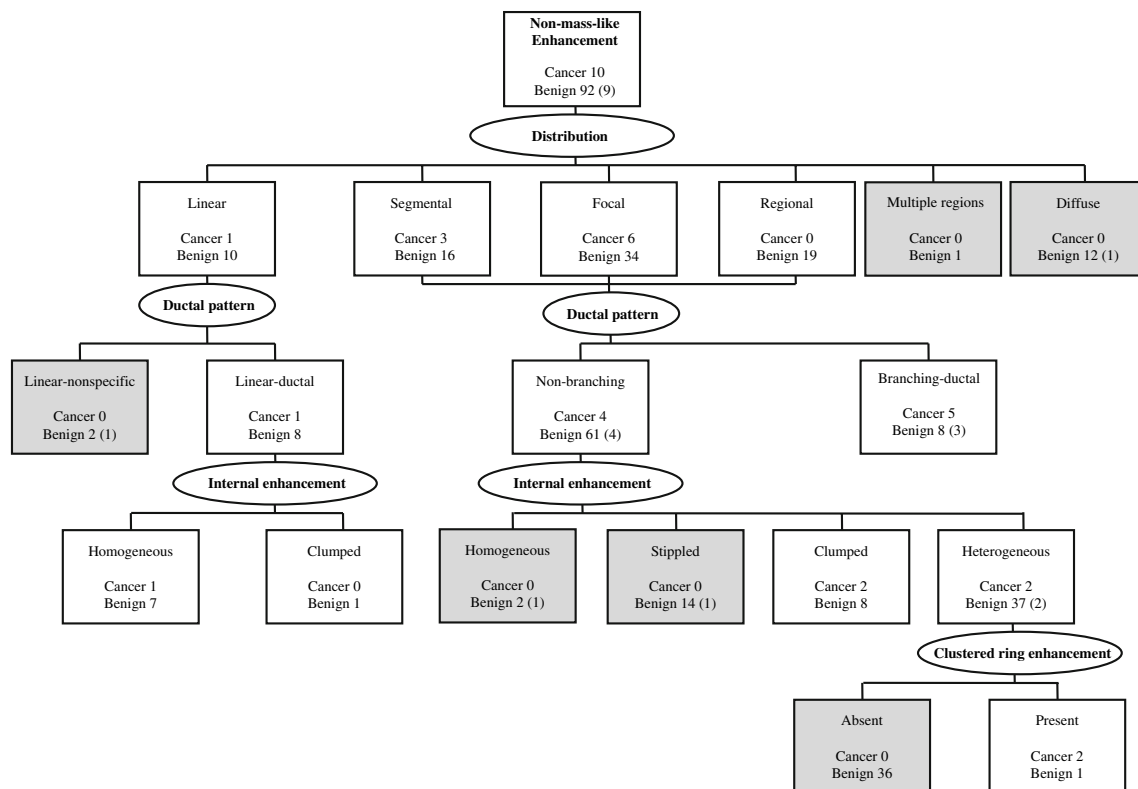


**Fig. 3** The interpretation model proposed by Tozaki et al. [11]. Benign terminal nodes are *shaded*. The cases of unsuccessful biopsy are shown in parentheses. All lesions showing multi-quadrant distribution (multiple regions, diffuse), linear-nonspecific lesion, non-

lesions. Morakkabati-Spitz et al. [10] reported that segmental enhancement was the most frequent manifestation of DCIS on dynamic MR imaging. In our results, none of the distribution patterns showed a statistically significant association with benign or malignant lesions. A focal distribution was the most frequent findings in malignant lesions (60%) and the PPV of segmental enhancement was only moderate (16%). We speculated that early-stage DCIS might not show segmental distribution. Although the distribution patterns were classified at first in the evaluation of the lesions, further assessment was made by evaluating the presence of a ductal pattern, clustered ring enhancement, and the evaluation of internal enhancement. The importance of distribution patterns in the assessment of MRI detected non-mass lesions might be relatively small. However, the significance of segmental distribution in these lesions should be demonstrated in prospective studies. Ultimately, we suggested that lesions with clustered ring enhancement, a branching-ductal pattern and clumped architecture should undergo biopsy (category 4). In this study, the PPV for cancer of a linear-ductal pattern was 11% (1/9). Liberman et al. [16] reported that the PPV of ductal enhancement was 26% (23/88). However, both linear- and branching-ductal lesions were included in their

branching pattern with homogeneous and stippled internal architecture, and heterogeneous lesion without clustered ring enhancement were diagnosed as benign

study [16]. The frequency of carcinoma for a linear-ductal lesion without branching pattern may be lower. Ultimately, we suggest that linear-ductal lesions should be followed carefully or evaluated by biopsy as needed (category 3b).

Moreover, all lesions showing multi-quadrant distribution (multiple regions, diffuse), linear-nonspecific lesion, non-branching pattern with homogeneous and stippled internal architectures, and heterogeneous lesion without clustered ring enhancement were diagnosed as benign. We found that these findings could be defined as probably benign findings (category 3a).

For MRI-detected lesions that can be seen on second-look US, biopsy can be performed under sonographic guidance. In this study, hypoechoic nodules or hypoechoic areas or ductlike structures were observed in the location of MRI-detected lesions in all cases. However, on the basis of MRI findings after biopsy, the success rate of US-VAB of the lesions was 91%. Second-look US failed to identify a sonographic correlation in 9% (9/102) of MRI-detected lesions. Concerning MRI-guided breast biopsy, several studies indicated that core needle biopsy and VAB could have high diagnostic yield. In the study by Kuhl et al. [17], MR-guided 14-gauge automated core biopsy was technically successful in 99% of cases (77/78). Perlet et al. [18]

reported that MRI-guided VAB was successfully performed in 517 (96%) of 538 women. Because VAB can be performed quickly, removes a large volume of tissue, provides more accurate characterization of lesions containing atypical ductal hyperplasia and DCIS, MRI-guided VAB may be necessary in Japan.

To the best of our knowledge, this is the first report of an interpretation model and categorization of lesions showing non-mass-like enhancement detected by MRI. However, only a relatively small group of 10 malignant lesions was evaluated. Therefore, further investigations and evaluations are needed to refine our interpretation model.

In conclusion, non-mass-like breast lesions detected on MRI showing a clustered ring enhancement, a branching-ductal pattern and clumped architecture should be evaluated further by biopsy (category 4), while other lesions not showing the aforementioned characteristics (category 3a) may be observed without unnecessary intervention. Lesions showing a linear-ductal pattern may be followed carefully or evaluated by biopsy as needed (category 3b).

## References

- Heywang SH, Wolf A, Pruss E, Hilbertz T, Eiermann W, Permanetter W. MR imaging of the breast with Gd-DTPA: use and limitations. *Radiology*. 1989;171:95–103.
- Kaiser WA, Zeitler E. MR imaging of the breast: fast imaging sequences with and without Gd-DTPA. *Radiology*. 1989;170:681–6.
- Harms SE, Flamig DP, Hesley KL, Meiches MD, Jensen RA, Evans WP, Savino DA, Wells RV. MR imaging of the breast with rotating delivery of excitation off resonance: clinical experience with pathologic correlation. *Radiology*. 1993;187:493–501.
- Orel SG, Schnall MD, LiVolsi VA, Troupin RH. Suspicious breast lesions: MR imaging with radiologic-pathologic correlation. *Radiology*. 1994;190:485–93.
- Boetes C, Barentsz JO, Mus RD, van der Sluis RF, van Erning LJ, Hendriks JH, Holland R, Ruys SH. MR characterization of suspicious breast lesions with a gadolinium-enhanced TurboFLASH subtraction technique. *Radiology*. 1994;193:777–81.
- Kuhl CK, Mielcareck P, Klaschik S, Leutner C, Wardelmann E, Gieseke J, Schild HH. Dynamic breast MR imaging: are signal intensity time course data useful for differential diagnosis of enhancing lesions? *Radiology*. 1999;211:101–10.
- Fischer U, Kopka L, Grabbe E. Breast carcinoma: effect of pre-operative contrast-enhanced MR imaging on the therapeutic approach. *Radiology*. 1999;213:881–8.
- American College of Radiology. Breast imaging reporting, data system (BI-RADS), 4th ed. Reston: American College of Radiology; 2003.
- Lieberman L, Morris EA, Lee MJ, Kaplan JB, LaTrenta LR, Menell JH, Abramson AF, Dashnaw SM, Ballon DJ, Dershaw DD. Breast lesions detected on MR imaging: features and positive predictive value. *AJR Am J Roentgenol*. 2002;179:171–78.
- Morakkabati-Spitz N, Leutner C, Schild H, Traeber F, Kuhl C. Diagnostic usefulness of segmental and linear enhancement in dynamic breast MRI. *Eur Radiol*. 2005;15:2010–7.
- Tozaki M, Fukuda K. High-Spatial-Resolution MRI of non-masslike breast lesions: interpretation model based on BI-RADS MRI descriptors. *AJR Am J Roentgenol*. 2006;187:330–7.
- Tozaki M, Igarashi T, Fukuda K. Breast MRI using the VIBE sequence: clustered ring enhancement in the differential diagnosis of lesions showing non-masslike enhancement. *AJR Am J Roentgenol*. 2006;187:313–21.
- Lazarus E, Mainiero MB, Schepps B, et al. BI-RADS lexicon for US and mammography: interobserver variability and positive predictive value. *Radiology*. 2006;239:385–91.
- Schnall MD, Ikeda DM. Lesion diagnosis working group on breast MR. *J Magn Reson Imaging*. 1999;10:982–90.
- Ikeda DM, Hylton NM, Kinkel K, Hochman MG, Kuhl CK, Kaiser WA, Weinreb JC, Smazal SF, Degani H, Viehweg P, Barclay J, Schnall MD. Development, standardization, and testing of a lexicon for reporting contrast-enhanced breast magnetic resonance imaging studies. *J Magn Reson Imaging*. 2001;13:889–95.
- Lieberman L, Morris EA, Dershaw DD, Abramson AF, Tan LK. Ductal enhancement on MR imaging of the breast. *AJR Am J Roentgenol*. 2003;181:519–25.
- Kuhl CK, Morakkabati N, Leutner CC, Schmiedel A, Wardelmann E, Schild HH. MR imaging-guided large-core (14-gauge) needle biopsy of small lesions visible at breast MR imaging alone. *Radiology*. 2001;220:31–9.
- Perlet C, Heywang-Kobrunner SH, Heinig A, Sittek H, Casselman J, Anderson I, Taourel P. Magnetic resonance-guided, vacuum-assisted breast biopsy: results from a European multicenter study of 538 lesions. *Cancer*. 2006;106:982–90.